The intrinsic energy of the gating isomerization of a neuromuscular acetylcholine receptor channel

Tapan K. Nayak, Prasad G. Purohit, and Anthony Auerbach

Department of Physiology and Biophysics, SUNY at Buffalo, Buffalo, NY 14214

Nicotinic acetylcholine receptor (AChR) channels at neuromuscular synapses rarely open in the absence of agonists, but many different mutations increase the unliganded gating equilibrium constant (E_0) to generate AChRs that are active constitutively. We measured E_0 for two different sets of mutant combinations and by extrapolation estimated E_0 for wild-type AChRs. The estimates were 7.6 and 7.8×10^{-7} in adult-type mouse AChRs (−100 mV at 23°C). The values are in excellent agreement with one obtained previously by using a completely different method (6.5×10^{-7}, from monoliganded gating). E_0 decreases with depolarization to the same extent as does the diliganded gating equilibrium constant, e-fold with ∼60 mV. We estimate that at −100 mV the intrinsic energy of the unliganded gating isomerization is +8.4 kcal/mol (35 kJ/mol), and that in the absence of a membrane potential, the intrinsic chemical energy of this global conformational change is +9.4 kcal/mol (39 kJ/mol). Na^+ and K^+ in the extracellular solution have no measureable effect on E_0, which suggests that unliganded gating occurs with only water occupying the transmitter binding sites. The results are discussed with regard to the energy changes in receptor activation and the competitive antagonism of ions in agonist binding.

The Journal of General Physiology

INTRODUCTION

Nicotinic acetylcholine receptors (AChRs) are ligand-gated ion channels that regulate the flux of cations across cell membranes by switching between closed- and open-channel conformations. This global change in AChR structure ("gating") occurs both with and without activating ligands ("agonists") present at the two extracellular transmitter binding sites. However, the gating equilibrium constant increases in the presence of agonists because these ligands bind with a higher affinity to the open-channel conformation of the protein.

To understand the energy that agonists provide for the full AChR gating isomerization, it is essential to link measurements of the equilibrium constants in both unliganded and fully liganded conditions in a thermodynamic cycle (Monod et al., 1965; Karlin, 1967; Jackson, 1986; Auerbach, 2010). The unliganded gating equilibrium constant (E_0) quantifies the tendency of the protein to adopt the high affinity/open conformation when no agonists are present at the binding sites, and the logarithm of E_0 gives the intrinsic energy of the gating conformational change. The extent to which each agonist molecule increases the gating equilibrium constant above this level is a measure of the energy it contributes toward the global conformational change of the protein. Having accurate estimates of this energy is one key to understanding how ligand binding and conformational change are coupled.

In pioneering experiments, Jackson (1984) used single-channel electrophysiology of mouse muscle and Neubig and Cohen (1980) used ion flux measurements of *Torpedo* electroplax membranes to estimate independently that the unliganded gating equilibrium constant of these AChRs is small, $\sim 10^{-7}$. More recently, we estimated E_0^{wt} for adult mouse neuromuscular AChRs (expressed in human embryonic kidney [HEK] cells; −100 mV) by using two different methods. By measuring single-channel currents in receptors having multiple gain-of-function background mutations, we estimated $E_0^{wt} \sim 1.2 \times 10^{-7}$ at −100 mV (Purohit and Auerbach, 2009). In these experiments, energy coupling between mutations was not taken into account, so this estimate is low. In the second method, E_0^{wt} was estimated from the ratio of the gating equilibrium constants of diliganded and monoliganded AChRs and was $\sim 6.5 \times 10^{-7}$ at −100 mV (Jha and Auerbach, 2010).

Here, we provide a new and more accurate estimate for E_0^{wt} in adult mouse neuromuscular AChRs (expressed in HEK cells), obtained by using an improved version of the gain-of-function background approach. We also explore the sensitivity of E_0 to membrane voltage and to the concentration of monovalent cations in the extracellular solution.

Correspondence to Anthony Auerbach: auerbach@buffalo.edu

Abbreviations used in this paper: AChR, acetylcholine receptor; Cho, choline; HEK, human embryonic kidney; R-E, rate–equilibrium; wt, wild type.

The Rockefeller University Press $30.00
J. Gen. Physiol. Vol. 139 No. 5 349–358
www.jgp.org/cgi/doi/10.1085/jgp.201110752

MATERIALS AND METHODS

Cell culture and mutagenesis

HEK 293 cells were maintained in Dulbecco's modified Eagle's medium supplemented with 10% fetal bovine serum and 1% penicillin–streptomycin, pH 7.4. The cultures were incubated at 37°C and 5% CO_2. Mutants of mouse AChR subunit cDNAs were made by using a site-directed mutagenesis kit (QuikChange; Agilent Technologies) and verified by nucleotide sequencing. HEK cells were transiently transfected using calcium phosphate precipitation by incubating them with 3.5–5.5 µg DNA per 35-mm culture dish in the ratio of 2:1:1:1 (α/β/δ/ε) for ∼16 h. Most electrophysiological experiments were done ∼24 h after transfection.

Electrophysiology

Single-channel currents were recorded at 23°C in the cell-attached patch configuration. The cells were bathed in K^+ Ringer's solution composed of (in mM): 142 KCl, 5.4 NaCl, 1.8 $CaCl_2$, 1.7 $MgCl_2$, and 10 HEPES/KOH, pH 7.4. The patch pipettes were generally filled with Dulbecco's PBS containing (in mM): 137 NaCl, 0.9 $CaCl_2$, 2.7 KCl, 1.5 KH_2PO_4, 0.5 $MgCl_2$, and 8.1 Na_2HPO_4, pH 7.3/NaOH. In experiments to study the effect of ions (Figs. 6 and S4), the pipette solution contained (in mM): 0–150 NaCl/KCl/CsCl, 0.9 $CaCl_2$, 0.5 $MgCl_2$, 1.5 KH_2PO_4, and 8.1 Na_2HPO_4. To study the effect of near complete ion removal on the receptor, the patch pipettes were filled with H_2O and 0.1 mM $CaCl_2$. In some experiments, the partial agonist choline (Cho) was added to the patch pipette solution.

Patch pipettes were fabricated from borosilicate glass, coated with sylgard (Corning), and fire polished to a resistance of ∼10 MΩ when filled with pipette solution. Single-channel currents were recorded using an amplifier (PC505; Warner Instruments). The single-channel records were low-pass filtered at 20 kHz and digitized at a sampling frequency of 50 kHz using a data acquisition board (SCB-68; National Instruments). The pipette holder used for the unliganded experiments was never exposed to agonists.

Selection and characterization of background

In wild-type (wt) AChRs, unliganded openings are very rare, so E_0^{wt} cannot be measured directly. We engineered two different sets of gain-of-function background mutation combinations to study unliganded gating. The first set of mutants, most of which had the background combination DYS (αD97A + αY127F + αS269I), were measured and described in detail previously (Purohit and Auerbach, 2009). In the second set, the key mutation was at αA96. Mutations here can increase the diliganded gating equilibrium constant with Cho (E_2^{Cho}) substantially and over a wide range (Cadugan and Auerbach, 2010). In addition, we used βT456I, δI43Q, εE181T, εL269F, and δV269A as background mutations in four different combinations. Individually, each of these mutations increases E_2^{Cho} (Table S1): βT456I, 2.1-fold (Mitra et al., 2004); δI43Q, 5.0-fold (see supplemental text); εE181T, 2.2-fold (Jha et al., 2012); εL269F, 179-fold (Jha et al., 2007); and δV269A, 250-fold (Cymes et al., 2002), in all cases by an almost equivalent increase in E_0.

We assumed that the effects of the individual mutations, as measured by E_2^{Cho}, were caused only by equivalent fold changes in E_0 and were approximately energetically independent of each other. For example, the product of the individual fold increases in E_2^{cho} for the background (βT456I + δI43Q + εL269F + εE181T) is 4135, and the individual fold increases for the αA96L and F mutants are 50 and 497. With the above assumptions, adding these to the background should result in a total increase in E_0 by factors of ∼0.21 and 2.1 million. The E_0^{obs} values for these final constructs were 0.11 and 1.37, which are approximately in the same ratio. This indicates that the energetic consequences of the αA96 mutations were approximately independent of those of the background.

Expression of most of the αA96 mutants was robust. In the absence of any agonists, the currents were ∼7 pA at −100 mV, and there was no channel block.

Kinetic modeling and determination of rate constants

Kinetic analyses of single-channel currents were done by using the QuB software suite (http://www.qub.buffalo.edu). For estimation of rate constants, clusters of individual channel activity, flanked by ≥20-ms nonconducting periods, were selected by eye. Clusters of unliganded activity were idealized into noise-free intervals after they were low-pass filtered digitally (12 kHz) by using the segmental K-means algorithm (Qin et al., 1996). The unliganded opening (f_0) and closing (b_0) rate constants were estimated from the idealized intra-cluster interval durations by using the maximum-interval likelihood (MIL) algorithm after imposing a dead time of 50 µs (Qin et al., 1997).

The kinetics of unliganded gating activity are complex (Jackson et al., 1990; Grosman and Auerbach, 2000b; Purohit and Auerbach, 2009). There were multiple components in the intra-cluster interval duration histograms. The idealized intra-cluster intervals were first fitted by a simple two-state closed (C)–open (O) model using the MIL algorithm. Additional C and O states were added, one at a time, until the log-likelihood score failed to improve by >10 units. The unliganded opening and closing rate constants (f_0 and b_0) were estimated from the inverse lifetimes of the predominant (≥80%) component of closed- and open-interval duration histograms. E_0, the unliganded gating equilibrium constant, was calculated as the ratio f_0/b_0. The fact that the slope of the E_0 plot (Fig. 2) was equal to 1 indicates that the above method consistently identified the same unliganded gating rate constants.

The unliganded activity of some αA96 background combinations exhibited distinct modes. In such cases, clusters were separated into populations based on their mean open probability, mean closed time, and mean open time using the "Select" feature and the K-means algorithm of QuB. The predominant (∼70%) gating mode was selected and E_0 was determined as described above.

Voltage dependence analysis

For unliganded gating, E_0 was measured at different membrane potentials (Fig. 5, A–D). Two different methods were used to estimate the voltage dependence of E_2. In some experiments, we assumed that low affinity agonist equilibrium dissociation constant was independent of voltage and measured an apparent diliganded opening rate constant (f_2*) and the diliganded closing rate constant (b_2) using 50–100 µM Cho. At these concentrations, channel block by Cho was minimal. In other experiments, we estimated f_2 using 20 mM Cho and b_2 using 100 µM Cho (Fig. 5, G and H).

To study the perturbation of voltage on gating, we plotted log f_0 (or f_2) versus log E_0 (or E_2) for eight different constructs (Fig. 5). This is a rate–equilibrium (R-E) relationship. The slope of this plot (Φ) was estimated by an unweighted linear fit in Sigmaplot 10 (Systat Software, Inc.). For a linear, sequential, bounded reaction mechanism, Φ may provide relative temporal information regarding the movement of the perturbed side chain in the gating reaction (1 is "early," 0 is "late," and the same is "synchronous") (Zhou et al., 2005).

Online supplemental material

The online supplemental material contains Tables S1–S5 and Figs. S1–S4. Tables S1 and S2 illustrate the effect of mutant combinations on the gating equilibrium constant. Tables S3 and S4

show the voltage dependence of the unliganded (E_0) and diliganded (E_2*) gating rates and equilibrium constants. Table S5 deals with the effect of cations on E_0. Fig. S1 shows the locations of the mutated amino acids in the *Torpedo* AChR (Protein Data Bank accession no. 2bg9). Fig. S2 presents the high resolution view of example unliganded currents for different αA96 mutants. The effects of membrane voltage and extracellular Cs^+ ions are shown in Figs. S3 and S4. The online supplemental material is available at http://www.jgp.org/cgi/content/full/jgp.201110752/DC1.

RESULTS

Theory and assumptions

A cyclic reaction scheme provides a useful, if approximate, description of AChR activation (Fig. 1). Without an external energy source, the product of the equilibrium constants linking the unliganded closed channel (R) and the diliganded open channel (A_2R*) is the same for the clockwise and anticlockwise connecting paths. Hence, with two equivalent binding sites (Akk et al., 1996; Salamone et al., 1999; Jha and Auerbach, 2010),

$$E_2 = E_0\lambda^2, \quad (1)$$

where E_2 is the diliganded gating equilibrium constant; E_0 is the unliganded gating equilibrium constant; and λ is the square root of their ratio or, equivalently, the ratio of low and high affinity equilibrium dissociation constants, K_d/J_d. The logarithm of λ quantifies the energy provided by each agonist molecule to power gating.

Many mutations throughout the AChR increase E_2, as measured using the partial agonist Cho (Grosman and Auerbach, 2000a; Chakrapani et al., 2004; Mitra et al., 2004; Spitzmaul et al., 2004; Purohit et al., 2007). According to Eq. 1, a mutation can increase E_2 by increasing E_0, λ, or both. The evidence suggests that many mutations that are not in the immediate vicinity of the transmitter binding sites that increase E_2^{Cho} do so by an approximately equivalent increase in E_0 and have little or no effect on λ (Jadey et al., 2011). These same experiments also show that these mutations often influence E_0 independently, because for many different mutant combinations, the net fold change in E_2^{Cho} is approximately the product of the fold changes for each mutation alone.

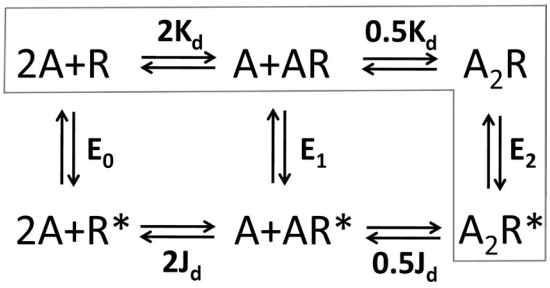

Figure 1. Cyclic reaction scheme for AChR binding and gating. A is the agonist, R is the resting conformation of the AChR (low affinity, closed channel), and R* is the active conformation (high affinity, open channel). K_d and J_d are the equilibrium dissociation constants of R and R*. E_0, E_1, and E_2 are the gating equilibrium constants with zero, one, and two bound agonist molecules. The logarithm of E_0 is the intrinsic energy for the protein isomerization in the absence of bound agonists. In wt AChRs, the unboxed states are rarely visited and only the boxed states determine physiological and pharmacological responses. The two transmitter binding sites are assumed to be functionally equivalent. Without an external energy source, the product of the equilibrium constants for the outer paths connecting R with A_2R* is equal ($E_2/K_d^2 = E_0/J_d^2$), so $E_2 = E_0\lambda^2$ where $\lambda = K_d/J_d$. A mutation that changes E_2 can do so by changing E_0, λ, or both.

These two characteristics of many AChR mutations—that they only change the intrinsic gating energy and act independently—offer a simple way to estimate the intrinsic gating energy of wt AChRs. First, measure the fold increase in E_2^{Cho} in AChRs having a side-chain substitution that increases the frequency of unliganded openings and assume that the increase is caused exclusively to a parallel increase in E_0 (that the mutation did not alter λ^{Cho}). Second, calculate what the predicted fold increase in E_2 would be for a combination of mutations (E_2^{mut}/E_2^{wt}) assuming that the effect of each mutation is energetically independent. That is, assume that the fold change in E_0 for the mutant combination is the product of the fold changes for each mutation alone. Third, express AChRs having the mutant combination and measure experimentally the unliganded gating equilibrium constant, E_0^{obs}. If the two assumptions are perfectly correct, then $E_0^{obs}/E_0^{wt} = E_2^{mut}/E_2^{wt}$. A log–log plot of E_0^{obs} versus E_2^{mut}/E_2^{wt} should be linear with a slope of 1 and an intercept on the ordinate axis, where $\log(E_2^{mut}/E_2^{wt}) = 0$, which is the estimate of $\log(E_0^{wt})$.

Estimates of E_0^{wt}

We used two different sets of background mutations to estimate E_0^{wt} in adult-type AChRs (Fig. S1). The first set was the same as reported previously but analyzed without considering the possibility that there was energy coupling between the mutations (Purohit and Auerbach, 2009). Many of the mutated amino acids in the first set were in the α subunit, close to each other and the transmitter binding site. For the second set, we chose fewer and more separated amino acids. The key mutation of the second set was at residue αA96. Side-chain substitutions here increase E_2^{Cho} over a wide range and, in some cases, to a great extent (Cadugan and Auerbach, 2010). As a consequence, only a few mutations were needed to generate the large increase in unliganded gating required to produce the clusters of spontaneous openings that are necessary for measuring E_0^{obs}.

Fig. 2 shows single-channel records of unliganded gating activity from example mutants of the second set. Without any agonists in the pipette or bath, openings occurred in clusters that each reflect the constitutive

gating activity of a single AChR. The gaps between clusters reflect epochs when all of the AChRs in the patch were desensitized. Different αA96 mutation increased the unliganded open probability of clusters to different extents. E_0^{obs} was measured for each mutant combination from the durations of shut and open intervals within clusters (see Materials and methods).

Log–log plots of E_0^{obs} versus E_2^{mut}/E_2^{wt} for both mutant sets are shown in Fig. 2 B. In both cases, the results were well described by a straight line over approximately four orders of magnitude. For the first mutant set, the extrapolated value was $E_0^{wt} = 7.8 \times 10^{-7}$ (95% confidence interval, 1.6–37 × 10^{-7}), and for the second set, it was $E_0^{wt} = 7.6 \times 10^{-7}$ (3.1–18 × 10^{-7}). The slope for the first set was 0.85 ± 0.1, and for the second it was 0.99 ± 0.07.

The slope for the first set was <1, which indicates that the two core assumptions of the method were not perfectly satisfied. In the first set, there was a small amount of energy coupling between the mutations, a small effect of some mutations on λ^{Cho} or both. Because the previous analysis of these mutants did not take into account such coupling, the new E_0^{wt} estimate was ∼6.5 times higher than the previous value. The slope of correlation for the second set was ∼1, so we conclude that there was essentially no energy coupling between these mutations.

Fig. 3 A shows unliganded gating activity from adult-type AChRs having only the αA96H substitution in both α subunits. This side-chain substitution alone was sufficient to raise unliganded gating activity to a level where clusters of spontaneous openings from individual AChRs were apparent. Fig. 3 B shows that adding a distant mutation (in the M4 helix of the β subunit) increased E_0^{obs} further and, hence, the probability of being open within unliganded clusters. This mutation increased E_2^{Cho} by increasing the opening rate constant by ∼1.1-fold and decreasing the closing rate constant by ∼2.1-fold (Mitra et al., 2004). In our experiments with unliganded AChRs, we found a similar result, namely that this mutation increased E_0^{obs} by increasing the opening rate constant by 1.8-fold and decreasing the closing rate constant by 2.2-fold.

In the absence of agonists, the intra-cluster interval duration distributions show multiple closed and open components (Jackson, 1986; Grosman and Auerbach, 2000b; Purohit and Auerbach, 2009). Recently, these "extra" states have been incorporated into a gating model that posits that the transmitter binding sites are energized ("primed") before channel opening, with brief versus long unliganded openings reflecting AChRs having one versus both sites so activated (Mukhtasimova et al., 2009). It is therefore important to consider whether

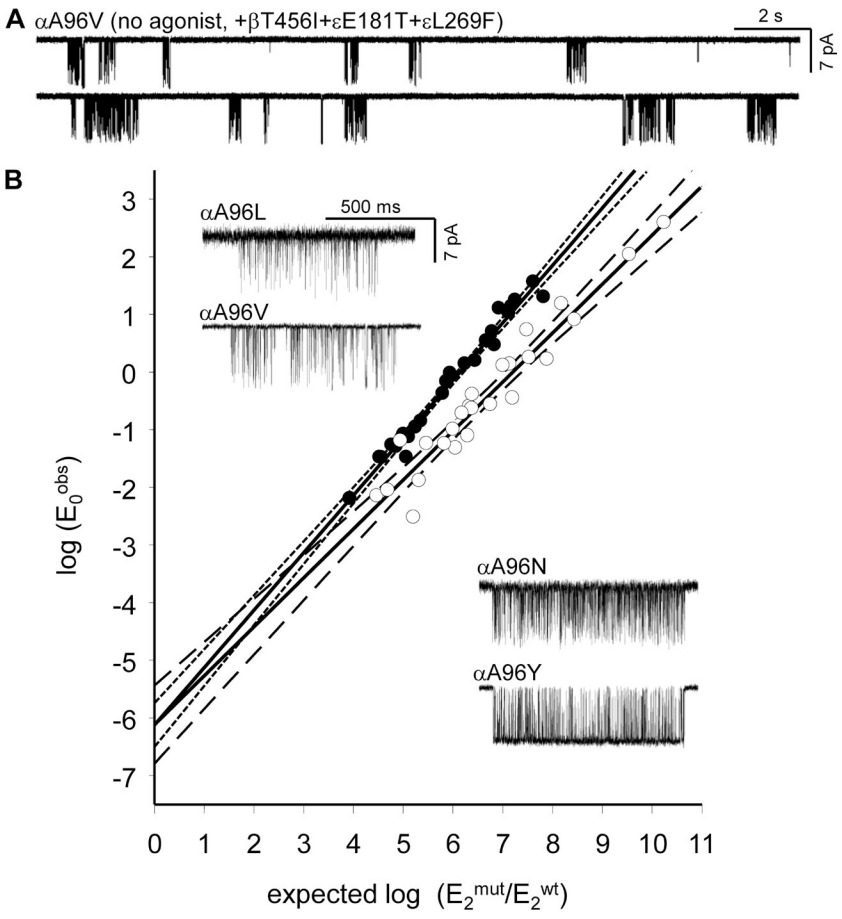

Figure 2. Estimating E_0^{wt} using mutations that increase the gating equilibrium constant. There was no agonist present in the pipette or bath. (A) Low time-resolution view of clusters of unliganded openings (open is down; −100 mV). Each cluster reflects the constitutive gating activity of an individual AChR. The background was βT456I + εE181T + εL269F (Table S1). (B) Estimation of the unliganded gating equilibrium constant of wt AChRs (E_0^{wt}) from different mutant sets (1, open; 2, closed). The data from set 1 are from Purohit and Auerbach (2009). The x-axis value is the log of the product of the fold increases in E_2^{Cho} for each mutation alone (Table S1), and the y axis is the log of E_0^{obs} measured directly from the clusters. For both mutant sets, the extrapolated ordinal intercept was approximately −6.12 (unweighted straight-line fit shown with 95% confidence intervals), which corresponds to $E_0^{wt} = \sim 7.6 \times 10^{-7}$. (Inset) Higher time-resolution view of clusters from mutant set 2 (αA96) expressed on the same background.

or not our association of the main component of each unliganded interval duration distribution with sojourns in the unliganded states of the cyclic model (R↔R* in Fig. 1) was appropriate.

Two previous results bear on this assessment. First, many point mutations of aromatic residues at the transmitter binding site eliminate the extra components apparent with the first mutant set and reduce unliganded gating to a simple two-state mechanism (Purohit and Auerbach, 2010). For example, the mutation αY198F, which removes only two oxygen atoms from the ∼300-kD AChR complex and has essentially no effect on diliganded gating, results in unambiguous R↔R* unliganded gating. Indeed, 55 of 57 mutations of the α-subunit–binding site aromatic residues (αY93, αY190, αY198, and αW149), and so far only of these four amino acids, completely eliminate the long component of unliganded openings.

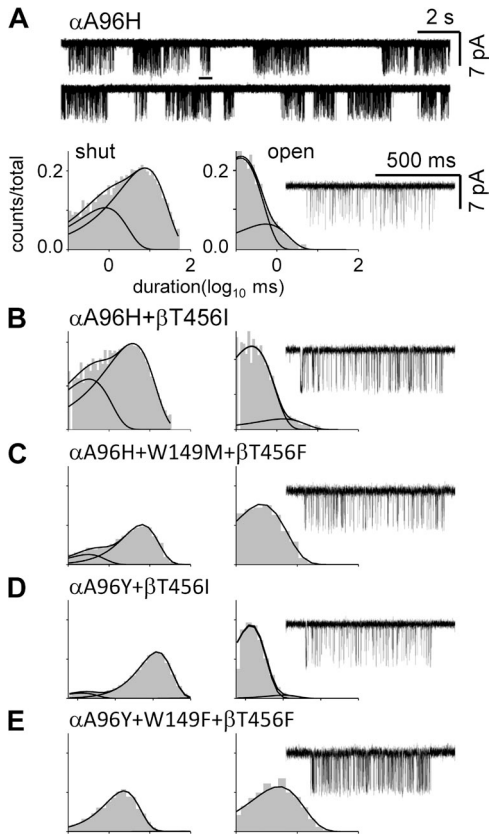

Figure 3. "Extra" shut and open components in unliganded gating. In all panels, there was no agonist present in the pipette or bath. (A; top) Continuous trace of clustered unliganded openings from AChRs having only the αA96H mutation (in both α subunits). This single mutation increases substantially E_0 and, hence, constitutive activity. (Bottom) Interval duration histograms of events within clusters and an example cluster (underlined, above). Two components are apparent in both the shut and open histograms. E_0^{obs} was estimated from the predominant components. (B) Adding the β-subunit M4 mutation βT456I increases E_0^{obs} but does not eliminate the extra components. (C) Adding the binding site mutation αW149M eliminates the long openings but has little effect on E_0^{obs}. (D) Another example of extra components in both the shut- and open-interval duration histograms. (E) These extra components disappear with the addition of the binding site mutation αW149F. After correcting for the backgrounds, the E_0 values were the same with or without the extra components.

We observed similar results using the αA96 background constructs. Fig. 3 C shows that with a construct from the second mutant set, the extra open component disappears when the αW149M mutation is added to the background. However, the E_0^{obs} estimate was similar without (0.04) or with (0.02) this added mutation. Fig. 3 D shows that multiple shut and open components are clearly apparent in the αA96Y background (used in mutant set 2) having the added βM4 mutation, but that these disappear with the addition of the αW149F mutation. Again, when the effect of the αW149F on E_0 is taken into account, the E_0^{obs} values were the same without and with (0.02) this mutation. Hence, for both the first and second mutant sets, the extra shut and open unliganded components are reduced by mutations of αW149, without influencing E_0^{obs} estimates.

A second previous observation regarding the extra unliganded components is that they are absent in currents generated by liganded AChRs (see Fig. 4 A). E_0^{wt} was estimated by examining ligand-gated currents from AChRs that had only one functional transmitter binding site (Jha and Auerbach, 2010). The results from these experiments, where no extra components were apparent and gating activity was unambiguously AR↔AR*, yielded a similar estimate of E_0^{wt} (for two different agonists) to that obtained from unliganded AChRs (6.5×10^{-7}).

Several additional results support the hypothesis that the main components of unliganded gating reflect the same conformational change as in diliganded gating and, hence, can be linked in a thermodynamic cycle. The liganded and unliganded R* conductances are the same (Jackson, 1984). The voltage dependences are the same (Fig. 5). Gating Φ values of many different residues are approximately the same with versus without ligands, which suggests that the conformational pathway connecting the R and R* end states is approximately the same (Purohit and Auerbach, 2009). The energy estimates calculated by using the cycle for the two ACh molecules (−10.2 kcal/mol) as well as the intrinsic isomerization (+8.4 kcal/mol; see below) are physically realistic. Collectively, the observations indicate that the association of the main shut and open components of unliganded gating with the R↔R* states of the cyclic model is appropriate.

Voltage dependence of the gating equilibrium constant

We next measured the voltage dependence of the gating equilibrium constant in both diliganded and unliganded AChRs (Fig. 4). Although the voltage dependence of the open-channel lifetime and the channel-closing rate constant in diliganded AChRs have been measured many times previously, estimates of the voltage dependence of the diliganded equilibrium constant are rarer (Colquhoun and Sakmann, 1985; Grosman et al., 2000).

To measure both the forward and backward gating rate constants in unliganded AChRs, we often needed to use background mutations that increased the opening rate constant and decreased the closing rate constant. In combination, these made it possible to measure intra-cluster closed- and open-interval durations over the range of −120 to +60 mV.

The results of these experiments are shown in Fig. 5 (Table S3). For both unliganded and diliganded conditions, and regardless of the background mutations, the gating equilibrium constant changed exponentially with membrane potential, decreasing on average e-fold with an ∼59 ± 6–mV depolarization (mean ± SD). These observations indicate that the background perturbations we used did not alter significantly the voltage sensitivity of the receptor. We estimate that in the absence of a membrane potential, $E_0^{wt,\ 0\ mV} = 1.3 \times 10^{-7}$.

We were also able to measure the extent to which the membrane potential changes the gating equilibrium constant by altering the forward versus the backward rate constant. The insets in Fig. 5 show this analysis in the form of R-E plots. For both the diliganded and unliganded conditions, and for all backgrounds, the predominant effect of depolarization was to increase the channel-closing rate constant. The average value of the slope of the eight R-E plots (Φ) for the voltage sensor was 0.34 ± 0.11.

Ion dependence of E_0

In the above experiments, the "unliganded" condition was AChRs exposed to the pipette solution without agonists, which was PBS (that contained 137 mM NaCl). Many AChR agonists are cations, so we considered the possibility that some or all of the constitutive activity observed in PBS might be attributed to extracellular Na^+ occupying the binding sites and acting as an agonist ($\lambda^{Na+} > 1$). To test this hypothesis, we removed all monovalent cations from the pipette solution (which contained only water and 0.1 mM $CaCl_2$) and clamped the cell membrane potential to +70 mV so that the currents flowed through the channel in an outward direction. The AChRs had the mutations αA96Y (to increase the frequency of unliganded openings) and δV269A (to prolong the open-channel lifetime). Fig. 6 A shows that AChRs still gave rise to clusters of spontaneous openings in the monovalent cation–free solution. The E_0 of the mutant in this condition was not significantly different from the E_0 observed under normal conditions with 137 mM Na^+ (Table S5). We exposed the AChRs in the patch to different concentrations of monovalent cations (Na^+, K^+, or Cs^+) in the pipette solution (the bath was K^+ Ringer's solution; see Materials and methods). Fig. 6 B shows that the pipette [Na^+] had no effect on E_0, and that the same result was observed when the Na^+ was replaced with K^+. The effect of pipette Cs^+ is described in the online supplemental material (Fig. S4 and Table S5).

DISCUSSION

All of the estimates of E_0^{wt}, obtained with different methods and different sets of background mutations, are in excellent agreement. Given the error limits on these measurements, we think a reasonable (and easily remembered) value for adult-type mouse neuromuscular

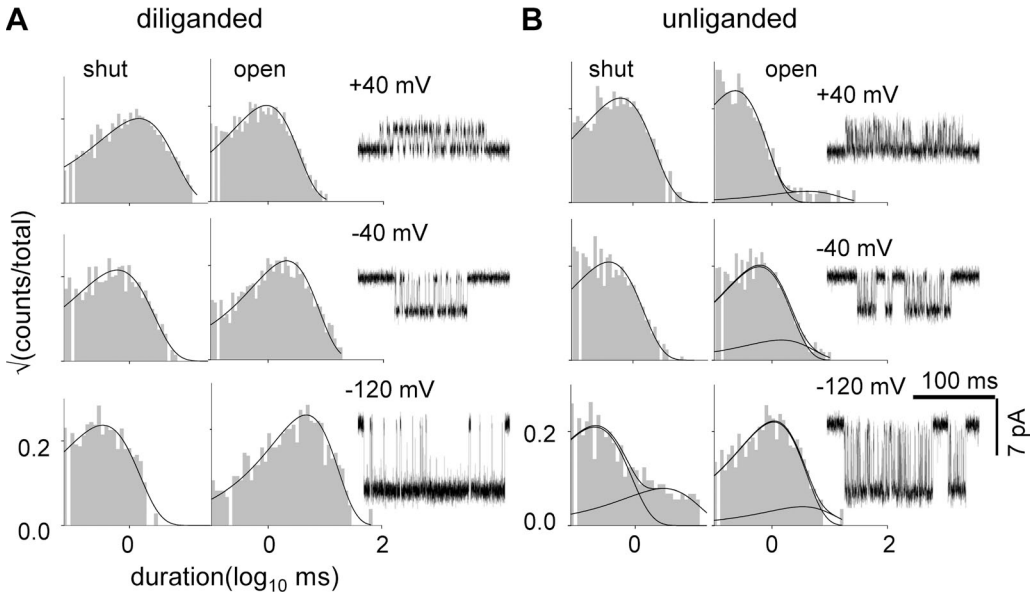

Figure 4. Interval duration histograms and example currents at different membrane potentials. (A) Diliganded gating activated by 50 µM Cho (the construct was αA96L + δV269A). (B) Unliganded gating (no agonist in the pipette or bath; the construct was αA96Y + δV269A). The extra components in the interval duration histograms in unliganded gating are not apparent in diliganded gating. Both with and without agonists, the shut lifetime decreases and the open lifetime increases with hyperpolarization.

AChRs is $E_0^{wt} = 7 \times 10^{-7}$ (−100 mV at 23°C). Mutations throughout the AChR can change E_0, so this value cannot be applied directly to any other receptor, for example, from a different species or one comprised of different subunits.

The logarithm of an equilibrium constant is proportional to the free energy difference between the end states. From the logarithm of E_0^{wt}, we estimate that at −100 mV, the intrinsic energy for the unliganded gating isomerization is +8.4 kcal/mol (35 kJ/mol). The electric field of the membrane contributes a modicum of energy for this conformational change. The gating equilibrium constant decreases e-fold with an ∼60-mV depolarization, so at zero membrane potential, $E_0^{wt} = 1.3 \times 10^{-7}$. We estimate that the intrinsic chemical energy of the mouse adult-type neuromuscular AChR-unliganded gating isomerization is +9.4 kcal/mol (39 kJ/mol).

With the new E_0^{wt} estimate, we can update the key equilibrium constants for adult AChR activation at −100 mV (Fig. 1). $E_2^{ACh} \approx 25$ (Wang et al., 2000; Hatton et al., 2003; Jadey et al., 2011), so, from the relationship $\lambda = \sqrt{(E_2/E_0)}$, we estimate that $\lambda^{ACh} \approx 6{,}000$. Each ACh molecule increases the gating equilibrium constant by this factor and provides approximately −5.1 kcal/mol (21.4 kJ) to power the gating isomerization of the protein. Together, the two binding sites provide −10.2 kcal/mol, which is sufficient to overcome the +8.4-kcal/mol intrinsic energy difference and, hence, open the channel with a high probability. With regard to transmitter binding, the low affinity equilibrium dissociation constant is $K_d^{ACh} \approx 166$ µM (Jadey et al., 2011), so we calculate (from the relationship $\lambda = K_d/J_d$) that the high affinity constant is $J_d^{ACh} \approx 28$ nM. Most of the extra energy from the agonist in the open conformation of the binding site is in the form of heat (Gupta and Auerbach, 2011).

We can separate the intrinsic gating free energy of unliganded gating ΔG^{E0} = +8.4 kcal/mol into enthalpy

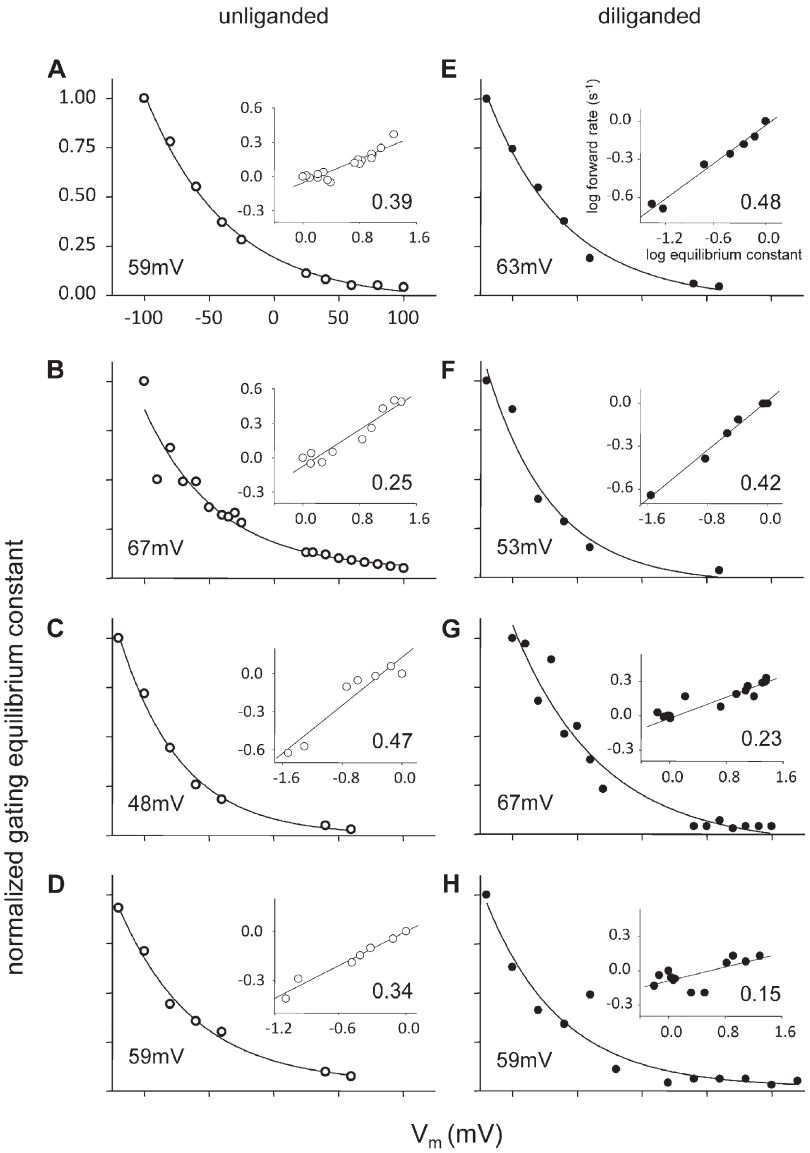

Figure 5. Voltage dependence of the gating equilibrium constant. (A–D) The unliganded gating equilibrium constant E_0 as a function of the membrane voltage (V_m) for different constructs. (Inset) Φ value analysis of the voltage sensor. (E–H) The diliganded gating equilibrium constant E_2 as a function of V_m for different mutants. Overall, there was an e-fold decrease in the gating equilibrium constant with a depolarization of 60 mV with Φ = 0.34. Unliganded constructs (no agonist): A, αDY + εL269F + εP245L; B, αDYS + δL265T and αDY + εL269F + εP245L; C, αA96Y + βT456I + δI43Q + εE181T + εL269F; D, αA96Y + δV269A. Diliganded constructs (activated by Cho): E, αA96L + δV269A; F, εE181T + εL269F; G, εL269F; H, εS450A.

(ΔH) and entropy (ΔS) components. The temperature dependence of E_2^{ACh} estimates the sum of the enthalpy changes for both the transmitter molecules and the intrinsic isomerization: $\Delta H^{E2(ACh)} = \Delta H^{ACh} + \Delta H^{E0}$. The experimental value was $\Delta H^{E2(ACh)}$ = +0.7 kcal/mol (Gupta and Auerbach, 2011). These same experiments showed that for different agonists, the differences in ΔG for diliganded gating was essentially equal to the differences in ΔH. Therefore, we postulate that $\Delta H^{ACh} = -10.2$ kcal/mol. We now calculate that $\Delta H^{E0} = +10.9$ kcal/mol, and, from the relationship $\Delta G = \Delta H - T\Delta S$ and the value $\Delta G^{E0} = +8.4$ kcal/mol, that $T\Delta S^{E0} = -2.5$ kcal/mol.

Many AChR mutations alter E_0 without changing K_d or λ, so many mutation-induced changes in cellular dose–response and kinetic profiles, including some that cause congenital myasthenic syndromes, can be traced specifically to changes in E_0 (Zhou et al., 1999). Indeed, it is remarkable that a single mutation in loop A of the α subunit (αA96H) increases E_0 by ∼100,000-fold (−6.8 kcal/mol) and by itself can lead to a relatively high frequency of opening in the absence of activating ligands (Fig. 3). This result is consistent with the previous suggestion that this region of loop A is acting as a "latch" that serves to hold the AChR in the low affinity, closed-channel conformation (Chakrapani et al., 2004).

The voltage dependence of E_0 is approximately the same as for E_2 (Fig. 5). The gating equilibrium constant decreases e-fold with an ∼60-mV depolarization, with or without agonists present at the binding sites. This result indicates that the product of the charge and displacement of the AChR voltage sensor is the same regardless of whether or not ligands occupy the transmitter binding sites. For all of the mutant combinations, the Φ value of the voltage sensor was low and similar with or without agonists, which is consistent with the proposal that the sequence of conformational changes within the complete gating isomerization is similar in liganded versus unliganded AChRs (Purohit and Auerbach, 2009).

We found no evidence that extracellular Na^+ or K^+ influences E_0. When added to the extracellular solution, these cations were without effect on unliganded gating (Fig. 6). Indeed, E_0 was the same without any monovalent cations as it was in PBS. We hypothesize that constitutive gating of AChRs occurs with only water present at the transmitter binding sites.

Extracellular Na^+ and K^+ are, however, competitive inhibitors of ACh association (Akk and Auerbach, 1996). There are two ways to reconcile this result with the lack of effect of these ions on E_0. It is possible that Na^+ and K^+ do indeed occupy the transmitter binding sites but experience no change in binding energy when the protein changes between its low and high affinity forms; i.e., perhaps $\lambda^{Na+} = 1$. This seems improbable. Other charged ligands experience a large energy change when the binding site switches its conformation. For example, tetramethylammonium ion experiences an approximately −4.0-kcal/mol energy change ($\lambda^{TMA} = 879$) in this switch (Zhang et al., 1995; Jadey et al., 2011). Also, the resolution of our experiments is approximately ±0.5 kcal/mol, so λ^{Na+} must be almost exactly 1 (between 0.4 and 2.3) to have no measureable effect on E_0, which is unlikely. Regardless, the above conclusion that unliganded gating occurs in water only is correct even if Na^+ (and K^+) does occupy the binding sites but has $\lambda \approx 1$.

A second possibility is that the competitive inhibition between ion and agonist occurs outside the binding site, before the low affinity complex has formed. Recently, we have found that low affinity binding to the AChR requires

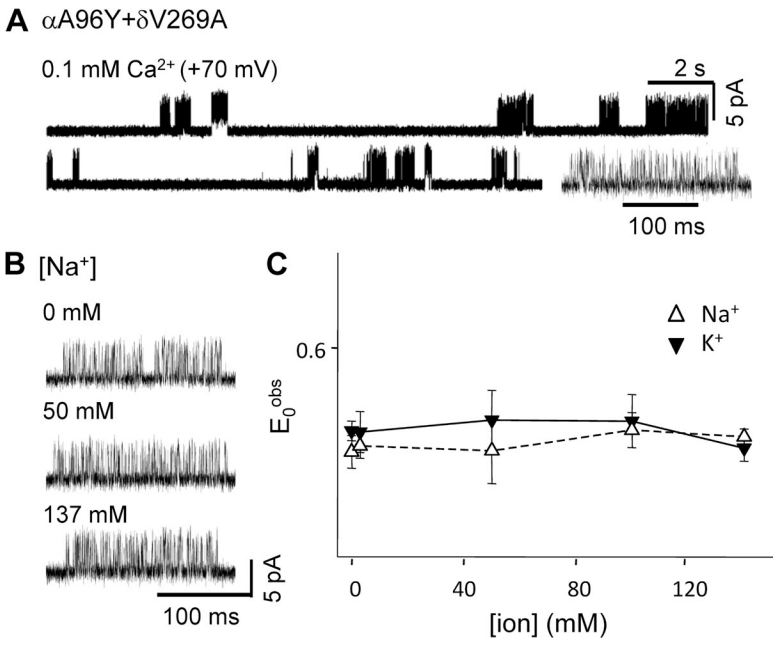

Figure 6. Effect of Na^+ and K^+ on E_0. (A) Spontaneous currents (no agonist in pipette or bath) at +70 mV (open is up). The pipette solution was only water plus 0.1 mM Ca^{2+}. (Bottom right) Marked cluster shown at higher resolution. (B) Effect of adding monovalent cations to the pipette solution. (Left) Unliganded current clusters with different amounts of extracellular Na^+. (C) The cluster open probability does not change with $[Na^+]$. (Right) E_0 was not influenced by $[Na^+]$ or $[K^+]$.

both diffusion and a protein conformational change (unpublished data). This implies that there is an "encounter complex" between agonist and protein that exists after the ligand has diffused to the binding site but before the conformational change has taken place. It is possible that Na^+ competes with ACh in the formation of this encounter complex rather than in low affinity binding. Further experiments are needed to reveal the basis of the competition between extracellular cations and agonists.

We would like to thank M. Teeling, M. Merritt, and M. Shero for technical assistance.

This work was supported by National Institutes of Health (grants R37-NS23513 and NS-064969).

Kenton J. Swartz served as editor.

Submitted: 12 December 2011
Accepted: 28 March 2012

REFERENCES

Akk, G., and A. Auerbach. 1996. Inorganic, monovalent cations compete with agonists for the transmitter binding site of nicotinic acetylcholine receptors. *Biophys. J.* 70:2652–2658. http://dx.doi.org/10.1016/S0006-3495(96)79834-X

Akk, G., S. Sine, and A. Auerbach. 1996. Binding sites contribute unequally to the gating of mouse nicotinic alpha D200N acetylcholine receptors. *J. Physiol.* 496:185–196.

Auerbach, A. 2010. The gating isomerization of neuromuscular acetylcholine receptors. *J. Physiol.* 588:573–586. http://dx.doi.org/10.1113/jphysiol.2009.182774

Cadugan, D.J., and A. Auerbach. 2010. Linking the acetylcholine receptor-channel agonist-binding sites with the gate. *Biophys. J.* 99:798–807. http://dx.doi.org/10.1016/j.bpj.2010.05.008

Chakrapani, S., T.D. Bailey, and A. Auerbach. 2004. Gating dynamics of the acetylcholine receptor extracellular domain. *J. Gen. Physiol.* 123:341–356. http://dx.doi.org/10.1085/jgp.200309004

Colquhoun, D., and B. Sakmann. 1985. Fast events in single-channel currents activated by acetylcholine and its analogues at the frog muscle end-plate. *J. Physiol.* 369:501–557.

Cymes, G.D., C. Grosman, and A. Auerbach. 2002. Structure of the transition state of gating in the acetylcholine receptor channel pore: a phi-value analysis. *Biochemistry.* 41:5548–5555. http://dx.doi.org/10.1021/bi011864f

Grosman, C., and A. Auerbach. 2000a. Asymmetric and independent contribution of the second transmembrane segment 12′ residues to diliganded gating of acetylcholine receptor channels: A single-channel study with choline as the agonist. *J. Gen. Physiol.* 115:637–651. http://dx.doi.org/10.1085/jgp.115.5.637

Grosman, C., and A. Auerbach. 2000b. Kinetic, mechanistic, and structural aspects of unliganded gating of acetylcholine receptor channels: A single-channel study of second transmembrane segment 12′ mutants. *J. Gen. Physiol.* 115:621–635. http://dx.doi.org/10.1085/jgp.115.5.621

Grosman, C., M. Zhou, and A. Auerbach. 2000. Mapping the conformational wave of acetylcholine receptor channel gating. *Nature.* 403:773–776. http://dx.doi.org/10.1038/35001586

Gupta, S., and A. Auerbach. 2011. Temperature dependence of acetylcholine receptor channels activated by different agonists. *Biophys. J.* 100:895–903. http://dx.doi.org/10.1016/j.bpj.2010.12.3727

Hatton, C.J., C. Shelley, M. Brydson, D. Beeson, and D. Colquhoun. 2003. Properties of the human muscle nicotinic receptor, and of the slow-channel myasthenic syndrome mutant epsilonL221F, inferred from maximum likelihood fits. *J. Physiol.* 547:729–760. http://dx.doi.org/10.1113/jphysiol.2002.034173

Jackson, M.B. 1984. Spontaneous openings of the acetylcholine receptor channel. *Proc. Natl. Acad. Sci. USA.* 81:3901–3904. http://dx.doi.org/10.1073/pnas.81.12.3901

Jackson, M.B. 1986. Kinetics of unliganded acetylcholine receptor channel gating. *Biophys. J.* 49:663–672. http://dx.doi.org/10.1016/S0006-3495(86)83693-1

Jackson, M.B., K. Imoto, M. Mishina, T. Konno, S. Numa, and B. Sakmann. 1990. Spontaneous and agonist-induced openings of an acetylcholine receptor channel composed of bovine muscle alpha-, beta- and delta-subunits. *Pflugers Arch.* 417:129–135. http://dx.doi.org/10.1007/BF00370689

Jadey, S.V., P. Purohit, I. Bruhova, T.M. Gregg, and A. Auerbach. 2011. Design and control of acetylcholine receptor conformational change. *Proc. Natl. Acad. Sci. USA.* 108:4328–4333. http://dx.doi.org/10.1073/pnas.1016617108

Jha, A., and A. Auerbach. 2010. Acetylcholine receptor channels activated by a single agonist molecule. *Biophys. J.* 98:1840–1846. http://dx.doi.org/10.1016/j.bpj.2010.01.025

Jha, A., D.J. Cadugan, P. Purohit, and A. Auerbach. 2007. Acetylcholine receptor gating at extracellular transmembrane domain interface: The cys-loop and M2–M3 linker. *J. Gen. Physiol.* 130:547–558. http://dx.doi.org/10.1085/jgp.200709856

Jha, A., S. Gupta, S.N. Zucker, and A. Auerbach. 2012. The energetic consequences of loop 9 gating motions in acetylcholine receptor-channels. *J. Physiol.* 590:119–129.

Karlin, A. 1967. On the application of "a plausible model" of allosteric proteins to the receptor for acetylcholine. *J. Theor. Biol.* 16:306–320. http://dx.doi.org/10.1016/0022-5193(67)90011-2

Mitra, A., T.D. Bailey, and A.L. Auerbach. 2004. Structural dynamics of the M4 transmembrane segment during acetylcholine receptor gating. *Structure.* 12:1909–1918. http://dx.doi.org/10.1016/j.str.2004.08.004

Monod, J., J. Wyman, and J.P. Changeux. 1965. On the nature of allosteric transitions: A plausible model. *J. Mol. Biol.* 12:88–118. http://dx.doi.org/10.1016/S0022-2836(65)80285-6

Mukhtasimova, N., W.Y. Lee, H.-L. Wang, and S.M. Sine. 2009. Detection and trapping of intermediate states priming nicotinic receptor channel opening. *Nature.* 459:451–454. http://dx.doi.org/10.1038/nature07923

Neubig, R.R., and J.B. Cohen. 1980. Permeability control by cholinergic receptors in Torpedo postsynaptic membranes: agonist dose-response relations measured at second and millisecond times. *Biochemistry.* 19:2770–2779. http://dx.doi.org/10.1021/bi00553a036

Purohit, P., and A. Auerbach. 2009. Unliganded gating of acetylcholine receptor channels. *Proc. Natl. Acad. Sci. USA.* 106:115–120. http://dx.doi.org/10.1073/pnas.0809272106

Purohit, P., and A. Auerbach. 2010. Energetics of gating at the apo–acetylcholine receptor transmitter binding site. *J. Gen. Physiol.* 135:321–331. http://dx.doi.org/10.1085/jgp.200910384

Purohit, P., A. Mitra, and A. Auerbach. 2007. A stepwise mechanism for acetylcholine receptor channel gating. *Nature.* 446:930–933. http://dx.doi.org/10.1038/nature05721

Qin, F., A. Auerbach, and F. Sachs. 1996. Estimating single-channel kinetic parameters from idealized patch-clamp data containing missed events. *Biophys. J.* 70:264–280. http://dx.doi.org/10.1016/S0006-3495(96)79568-1

Qin, F., A. Auerbach, and F. Sachs. 1997. Maximum likelihood estimation of aggregated Markov processes. *Proc. Biol. Sci.* 264:375–383. http://dx.doi.org/10.1098/rspb.1997.0054

Salamone, F.N., M. Zhou, and A. Auerbach. 1999. A re-examination of adult mouse nicotinic acetylcholine receptor channel activation

kinetics. *J. Physiol.* 516:315–330. http://dx.doi.org/10.1111/j.1469-7793.1999.0315v.x

Spitzmaul, G., J. Corradi, and C. Bouzat. 2004. Mechanistic contributions of residues in the M1 transmembrane domain of the nicotinic receptor to channel gating. *Mol. Membr. Biol.* 21:39–50. http://dx.doi.org/10.1080/09687680310001607341

Wang, H.L., K. Ohno, M. Milone, J.M. Brengman, A. Evoli, A.P. Batocchi, L.T. Middleton, K. Christodoulou, A.G. Engel, and S.M. Sine. 2000. Fundamental gating mechanism of nicotinic receptor channel revealed by mutation causing a congenital myasthenic syndrome. *J. Gen. Physiol.* 116:449–462. http://dx.doi.org/10.1085/jgp.116.3.449

Zhang, Y., J. Chen, and A. Auerbach. 1995. Activation of recombinant mouse acetylcholine receptors by acetylcholine, carbamylcholine and tetramethylammonium. *J. Physiol.* 486:189–206.

Zhou, M., A.G. Engel, and A. Auerbach. 1999. Serum choline activates mutant acetylcholine receptors that cause slow channel congenital myasthenic syndromes. *Proc. Natl. Acad. Sci. USA.* 96:10466–10471. http://dx.doi.org/10.1073/pnas.96.18.10466

Zhou, Y., J.E. Pearson, and A. Auerbach. 2005. Φ-value analysis of a linear, sequential reaction mechanism: theory and application to ion channel gating. *Biophys. J.* 89:3680–3685. http://dx.doi.org/10.1529/biophysj.105.067215